



# Adaptive hierarchical sliding mode control using neural network for uncertain 2D overhead crane

Hai Xuan Le<sup>1</sup> · Thai Van Nguyen<sup>2</sup> · Anh Viet Le<sup>2</sup> · Tuan Anh Phan<sup>2</sup> · Nam Hoai Nguyen<sup>2</sup> · Minh Xuan Phan<sup>2</sup>

Received: 3 August 2018 / Revised: 2 January 2019 / Accepted: 15 February 2019  
© Springer-Verlag GmbH Germany, part of Springer Nature 2019

## Abstract

This paper proposes an adaptive hierarchical sliding mode control method based on radial basis function neural network for an uncertain 2D overhead crane system. A second-level sliding surface is defined by a linear combination of two subsystem's sliding surfaces. A radial basis function neural network is adopted to approximate the unknown dynamic model. The control law is designed in order to ensure the stability of sliding surfaces and an updated law for neural network's weight matrices is derived from a candidate of Lyapunov function. Simulation results show that the effectiveness of the proposed control scheme, such as smaller swing and accurate position as desired. Besides that, the controller is installed in micro-controller for the actual model in laboratory and experiment result evaluate the applicability of this control design in industrial applications.

**Keywords** 2D overhead crane · Adaptive hierarchical sliding mode control · Neural network · Radial basis function

## 1 Introduction

Overhead crane is essential load or unload equipment, widely used in many areas such as at construction sites, factories, and harbors. The model of a crane belongs to a class of underactuated mechanical systems, with one control input (a trolley driving force) and two system variables to be controlled (the trolley position and the swing angle of payload). That leads to the unexpected swing of payload in operation which can cause dangers to workers or destroy surrounding devices. Therefore, the control objective of the crane is to move trolley on the desired path and make the payload oscillation as

smallest as possible. Research on enhancing the quality and reliability of the control crane system has been scrutinized and developed by many researchers.

Various attempts for control of the overhead crane have been proposed, concentrate on methods because it ensures the precision of motions using the feedback states. For example, Fang et al. [1] investigated three different controllers that include proportional-derivative control law and two coupling designs based on squared energy and kinetic energy for a 3D crane. A nonlinear feedback technique was utilized in [2], where the control signal contains a slow component to ensure the payload track a reference and a fast supplement to eliminate oscillations. In [3], the authors investigated the feedback linearization method and its application in control of a 2D crane with hoisting motion. Le et al. [4, 5] used partial feedback linearization to design a scheme which was a combination of two portions obtained from the feedback linearization of the actuated and un-actuated states. Several other studies concerned the approaches using fuzzy logic inference [6–8] due to the advantage that there is no requirement about accurate system modeling when designing control scheme.

Besides the aforementioned control methods, sliding mode control, which is regarded as a robust and effective technique, was applied in many non-linear control problems [9–13]. For a class of underactuated systems like the overhead crane, the issue related to defining sliding surfaces and

✉ Tuan Anh Phan  
anhantuanphan2510@gmail.com

Hai Xuan Le  
xhaicuw.edu.vn@gmail.com

Thai Van Nguyen  
thai.nguyenvan9495@gmail.com

Anh Viet Le  
anhvietlee0101@gmail.com

Nam Hoai Nguyen  
nam.nguyenhoai@hust.edu.vn

Minh Xuan Phan  
minh.phanxuan@hust.edu.vn

<sup>1</sup> College of Urban Works Construction, Hanoi, Vietnam

<sup>2</sup> Hanoi University of Science and Technology, Hanoi, Vietnam

ensuring stability is a difficult task due to the requirement of preserving the stability of two subsystems with only one control signal. Various definitions of sliding surfaces have been presented, for example, in [9] and [11], the sliding surface was defined as a linear combination of two components include the sliding surface of actuated states and the error of un-actuated ones, or in studies [10] and [14], an intermediate variable was determined as a linear combination of state errors, then second-level surface was defined based on intermediate variable.

The hierarchical sliding mode control (HSMC), a typical type of sliding mode control which is especially suitable for a class of underactuated systems, was published in recent studies [15] and [16]. Wang et al. [15] proposed HSMC structure for a class of second-order underactuated systems, which is divided into two subsystems based on control target, then a first-level sliding surface of each subsystem is defined. A second-level sliding surface was determined as a combination of these first-level sliding surfaces and utilized to design control law. In [17], Wang et al. not only extended the applied ranged of the method in [15] for a class of SIMO underactuated systems but also developed another structure of hierarchical sliding mode control, where sliding surface of the first subsystem was defined as first-layer sliding surface, then this sliding surface was combined with the sliding surface of the second subsystem in order to construct the second-layer sliding surface. This process continues until the sliding surface of the last subsystem. Moreover, the stability of all subsystem surfaces when using HSMC was proved in that article. HSMC structure was applied to the overhead crane system in [18] and the simulation results verify the quality of that control method. In [19], the HSMC structure was used together with fast terminal sliding surface definition to enable finite-time convergence to equilibrium closed-loop system.

On the other hand, due to the fact that there exist variations of system parameters as well as input disturbances, many researchers considered to design adaptive control laws that uncertainties of the system are estimated. In [20] and [21], adaptive control laws were presented, in which unknown parameters of the crane are updated and experiment results show the performance of these methods. Besides, numerous works attempt to integrate the approximation using artificial neural network for fuzzy-logic systems into conventional non-linear control laws. In [22], the authors used the dynamic surface control to create the frame of controller, then used the output of radial basis function network to represent the uncertain dynamical terms. In [23] and [24], a fuzzy uncertainty observer was employed to represent the system uncertainties as well as actuator nonlinearity. Hung et al. [25, 26] considered control methods for a class of nonlinear systems which contained unknown functions estimated by neural network and fuzzy-neural network. In [27], Huang et al. proposed an adaptive control strategy for a three degree-of-freedom

dynamic absorber system using sliding mode control scheme and RBF network. In [28], the authors use RBF network to constitute an approximation, in which two dynamical functions were estimated online, and traditional sliding mode control to design the control law for offshore container crane. Nevertheless, most of the previous studies have developed the theoretical control laws and verified through simulation. The capability of implementing the neural-based adaptive law on the real-time applications have not been mentioned.

Due to the aforementioned analysis, in this work, an adaptive hierarchical sliding mode control (AHSMC) was investigated to solve the experiment-oriented control problem of the 2D overhead crane. Hierarchical sliding mode control (HSMC) is utilized to create the frame of controller, in which sliding surface in the second layer is determined as a linear combination of sliding surfaces of the two subsystems. Meanwhile, all four non-linear dynamical functions of the overhead crane are estimated by RBF network to cope with external disturbance and parametric uncertainties. The simulation results for the HSMC and AHSMC control laws are compared to evaluate the performance of those. More importantly, the AHSMC controller is implemented on micro-controller to control the overhead crane prototype in laboratory, and the experimental results emphasize that the controller still guarantees the system robustness in case of large variation of parameters and disturbances. Furthermore, the proposed method also reduces the amount of work when applying in various different environments due to the advantage that there is no need to adequately describe the model of system.

This paper is divided into five parts: Introduction, Hierarchical sliding mode control for overhead crane, Adaptive hierarchical sliding mode control based on neural network, Simulation and experiment results, and Conclusion.

## 2 Hierarchical sliding mode control for overhead crane

### 2.1 Dynamic model of 2D overhead crane

Figure 1 illustrates the diagram of a 2D overhead crane, that includes trolley and payload. Trolley and payload are considered like moving on  $Oxy$  plane. We assume that static friction is non-exist, the rope is inflexible, the rope mass is ignored and the trolley and the payload are considered as material particles.

Mathematical model of 2D overhead crane is described as follows [7]:

$$\begin{aligned}(M + m)\ddot{x} + m\ddot{\theta} \cos \theta - m\dot{\theta}^2 \sin \theta &= F \\ \ddot{\theta} + g \sin \theta + \ddot{x} \cos \theta &= 0\end{aligned}\quad (1)$$

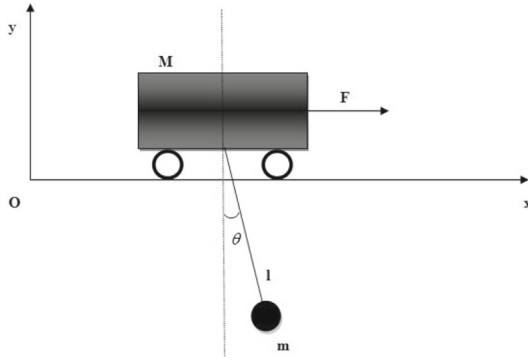


Fig. 1 Overhead crane system

where  $M$  is trolley mass,  $m$  is payload mass,  $l$  is rope length,  $g$  is gravitational acceleration,  $\theta$  is swing angle of the payload with respect to the vertical line,  $x$  is position of the trolley with respect to the origin,  $F$  is drive force applied to the trolley.

Defining  $u = F$  and the state vector as  $X^T = [x_1 \ x_2 \ x_3 \ x_4] = [x \ \dot{x} \ \theta \ \dot{\theta}]$ , the motion Eq. (1) can be transformed to the state space expression as:

$$\begin{aligned} \dot{x}_1 &= x_2 \\ \dot{x}_2 &= f_1(X) + g_1(X)u \\ \dot{x}_3 &= x_4 \\ \dot{x}_4 &= f_2(X) + g_2(X)u \end{aligned} \quad (2)$$

Here  $f_1$ ,  $g_1$ ,  $f_2$  and  $g_2$  are as follows:

$$\begin{aligned} f_1(X) &= \frac{ml\dot{\theta}^2 \sin \theta + mg \sin \theta \cos \theta}{M + m \sin^2 \theta} \\ g_1(X) &= \frac{1}{M + m \sin^2 \theta} \\ f_2(X) &= -\frac{(M + m)g \sin \theta + ml\dot{\theta}^2 \sin \theta \cos \theta}{(M + m \sin^2 \theta)l} \\ g_2(X) &= -\frac{\cos \theta}{(M + m \sin^2 \theta)l} \end{aligned}$$

## 2.2 Hierarchical sliding mode control

Hierarchical sliding mode control method which was proposed by Qian et al. [16] is an appropriate approach for a class of underactuated systems. In this section, HSMC is designed for the 2D overhead crane. Control law is constructed based on Lyapunov theory to ensure sliding surfaces's stability.

Defining error vector

$$e(t) = \begin{bmatrix} x_1 - x_d \\ x_3 - \theta_d \end{bmatrix} = \begin{bmatrix} x - x_d \\ \theta - \theta_d \end{bmatrix} = \begin{bmatrix} e_1 \\ e_3 \end{bmatrix}$$

where  $x_d$  and  $\theta_d$  desired position and desired swing angle. It is assumed that  $\dot{x}_d$  is exist and bounded, then Eq. (2) can be rewritten as:

$$\begin{aligned} \dot{e}_1 &= e_2 \\ \dot{e}_2 &= f_1(X) + g_1(X)u - \ddot{x}_d \\ \dot{e}_3 &= e_4 \\ \dot{e}_4 &= f_2(X) + g_2(X)u \end{aligned} \quad (3)$$

Firstly, first-level sliding surfaces of subsystems are defined as:

$$\begin{aligned} s_1 &= c_1 e_1 + e_2 \\ s_2 &= c_2 e_3 + e_4 \end{aligned} \quad (4)$$

where  $c_1$  and  $c_2$  are positive constants.

Next, the second-level sliding surface is constructed as a linear combination of two first-level sliding surfaces:

$$s = \alpha s_1 + \beta s_2 \quad (5)$$

From (4) and (5) we obtain the derivative of second-level sliding surface:

$$\begin{aligned} \dot{s} &= \alpha \dot{s}_1 + \beta \dot{s}_2 \\ &= \alpha(c_1 \dot{e}_1 + \dot{e}_2) + \beta(c_2 \dot{e}_3 + \dot{e}_4) \\ &= \alpha(c_1 e_2 + f_1 + g_1 u - \ddot{x}_d) \\ &\quad + \beta(c_2 e_4 + f_2 + g_2 u) \end{aligned} \quad (6)$$

Based on the methodology of equivalent control of variable structure control, total control law include two parts as follows:

$$u = u_{eq} + u_{sw} \quad (7)$$

Considering Lyapunov function candidate  $V = \frac{1}{2}s^2$ . Differentiating  $V$  with respect to time, we obtain:

$$\begin{aligned} \dot{V} &= s\dot{s} \\ &= s(\alpha(c_1 e_2 + f_1 + g_1 u - \ddot{x}_d) \\ &\quad + \beta(c_2 e_4 + f_2 + g_2 u)) \\ &= s(\alpha c_1 e_2 + \beta c_2 e_4 + \alpha f_1 + \beta f_2 - \alpha \ddot{x}_d \\ &\quad + (\alpha g_1 + \beta g_2)u) \end{aligned} \quad (8)$$

In order to ensure the stability of second-level sliding surface, let:

$$\begin{aligned} (\alpha g_1 + \beta g_2)u_{eq} + \alpha c_1 e_2 + \beta c_2 e_4 + \alpha f_1 + \beta f_2 - \alpha \ddot{x}_d &= 0 \\ (\alpha g_1 + \beta g_2)u_{sw} + k_1 s + k_2 \text{sgn}(s) &= 0 \end{aligned} \quad (9)$$

be the equivalent law and switching law, where  $k_1$  and  $k_2$  are positive constants.

From (7) and (9), we obtain control signal that given by:

$$u = -(\alpha c_1 e_2 + \alpha f_1 + \beta c_2 e_4 + \beta f_2 - \alpha \ddot{x}_{1d} + k_1 s + k_2 \text{sgn}(s)) / (\alpha \hat{g}_1 + \beta \hat{g}_2) \quad (10)$$

Substituting (10) into (9) we have

$$\dot{V} = s\dot{s} = s(-k_1 s - k_2 \text{sgn}(s)) = -k_1 s^2 - k_2 |s| \leq 0$$

### 3 Adaptive hierarchical sliding mode control based on neural network

In this section, based on HSMC structure, which is presented in section II, an AHSMC law for uncertain overhead crane using RBFNN is designed and the stability of closed-loop system is analysed.

#### 3.1 Control law design

Considering mathematical model of error state (3), in which four dynamical functions of system  $f_1(X)$ ,  $g_1(X)$ ,  $f_2(X)$  and  $g_2(X)$  are unknown, where  $X = [x \ \dot{x} \ \theta \ \dot{\theta}]^T \in \Omega_X \subset R^4$ , with  $\Omega_X$  being a known compact set. RBF network is utilized to approximate  $f_1(X)$ ,  $g_1(X)$ ,  $f_2(X)$  and  $g_2(X)$  as follows:

$$\begin{aligned} f_1(X) &= W_1^T \underline{h}(X) + \varepsilon_1(X) \\ g_1(X) &= W_2^T \underline{h}(X) + \varepsilon_2(X) \\ f_2(X) &= W_3^T \underline{h}(X) + \varepsilon_3(X) \\ g_2(X) &= W_4^T \underline{h}(X) + \varepsilon_4(X) \end{aligned} \quad (11)$$

where  $W_i(X)$ ;  $i = 1, 2, 3, 4$  is an ideal weight matrix,  $|\varepsilon_i(X)| \leq \varepsilon_i$   $i = 1, 2, 3, 4$  is the approximation error with constants  $\varepsilon_i > 0$ .

Defining  $\hat{W}_1, \hat{W}_2, \hat{W}_3$  and  $\hat{W}_4$  as estimations of  $W_1, W_2, W_3$  and  $W_4$ , respectively,  $\hat{f}_1, \hat{g}_1, \hat{f}_2$  and  $\hat{g}_2$  as estimations of  $f_1, g_1, f_2$  and  $g_2$ , respectively. The outputs of RBF networks are an approximation of real uncertain functions which are determined as follow:

$$\begin{aligned} \hat{f}_1(X) &= \hat{W}_1^T \underline{h}(X) \\ \hat{g}_1(X) &= \hat{W}_2^T \underline{h}(X) \\ \hat{f}_2(X) &= \hat{W}_3^T \underline{h}(X) \\ \hat{g}_2(X) &= \hat{W}_4^T \underline{h}(X) \end{aligned} \quad (12)$$

Considering a Lyapunov function candidate as follows:

$$V = \frac{1}{2} \left( s^2 + \sum_{i=1}^4 \tilde{W}_i^T F_i^{-1} \tilde{W}_i \right) \quad (13)$$

with  $\tilde{W}_i = W_i - \hat{W}_i$  is the error of weight matrix.

Differentiating the Lyapunov function (13) with respect to time and after some calculations, we obtain:

$$\begin{aligned} \dot{V} &= s\dot{s} + \sum_{i=1}^4 \tilde{W}_i^T F_i^{-1} \dot{\tilde{W}}_i \\ &= s \left( \begin{aligned} &\alpha c_1 e_2 + \alpha \hat{f}_1 + \beta c_2 e_4 \\ &+ \beta \hat{f}_2 - \ddot{x}_{1d} + (\alpha \hat{g}_1 + \beta \hat{g}_2) u \end{aligned} \right) \\ &\quad + s \left( \begin{aligned} &\alpha (\tilde{W}_1^T \underline{h} + \varepsilon_1) + \beta (\tilde{W}_3^T \underline{h} + \varepsilon_3) \\ &+ \alpha u (\tilde{W}_2^T \underline{h} + \varepsilon_2) + \beta u (\tilde{W}_4^T \underline{h} + \varepsilon_4) \end{aligned} \right) \\ &\quad + \sum_{i=1}^4 \tilde{W}_i^T F_i^{-1} \dot{\tilde{W}}_i \end{aligned} \quad (14)$$

The control signal  $u$  of the AHSMC law is determined as follows:

$$u = -(\alpha c_1 e_2 + \alpha \hat{f}_1 + \beta c_2 e_4 + \beta \hat{f}_2 - \ddot{x}_{1d} + k_1 s + k_2 \text{sgn}(s)) / (\alpha \hat{g}_1 + \beta \hat{g}_2) \quad (15)$$

Substituting (15) into (14):

$$\begin{aligned} \dot{V} &= -k_1 s^2 - k_2 |s| + \tilde{W}_1^T (\alpha s \underline{h} - F_1^{-1} \dot{\tilde{W}}_1) \\ &\quad + \tilde{W}_2^T (\alpha u s \underline{h} - F_2^{-1} \dot{\tilde{W}}_2) + \tilde{W}_3^T (\beta s \underline{h} - F_3^{-1} \dot{\tilde{W}}_3) \\ &\quad + \tilde{W}_4^T (\beta u s \underline{h} - F_4^{-1} \dot{\tilde{W}}_4) \\ &\quad + s(\alpha \varepsilon_1 + \beta \varepsilon_3 + \alpha u \varepsilon_2 + \beta u \varepsilon_4) \end{aligned} \quad (16)$$

Adaptive laws for weight matrices  $\hat{W}_1, \hat{W}_2, \hat{W}_3$  and  $\hat{W}_4$  are selected as:

$$\begin{aligned} \dot{\hat{W}}_1 &= F_1 (\alpha s \underline{h} - \eta |s| \hat{W}_1) \\ \dot{\hat{W}}_2 &= F_2 (\alpha u s \underline{h} - \eta |s| \hat{W}_2) \\ \dot{\hat{W}}_3 &= F_3 (\beta s \underline{h} - \eta |s| \hat{W}_3) \\ \dot{\hat{W}}_4 &= F_4 (\beta u s \underline{h} - \eta |s| \hat{W}_4) \end{aligned} \quad (17)$$

where  $F_1, F_2, F_3, F_4$  and  $\eta$  are positive constants.

The adaption mechanism (17) leads the derivative with respect to time of the Lyapunov function (16) to:

$$\begin{aligned} \dot{V} = & -k_1 s^2 - k_2 |s| + \eta |s| \sum_{i=1}^4 \tilde{W}_i^T (W_i - \tilde{W}_i) \\ & + s(\alpha \varepsilon_1 + \beta \varepsilon_3 + \alpha u \varepsilon_2 + \beta u \varepsilon_4) \end{aligned} \quad (18)$$

Using Cauchy–Schwarz inequality as:

$$\begin{aligned} \sum_{i=1}^4 \tilde{W}_i^T (W_i - \tilde{W}_i) & \leq \sum_{i=1}^4 \|\tilde{W}_i\| \left( \|W_i\| - \|\tilde{W}_i\| \right) \\ & = -\sum_{i=1}^4 \left( \|\tilde{W}_i\| - \frac{1}{2} \|W\| \right)^2 + \frac{1}{4} \eta |s| \sum_{i=1}^4 \|W_i\|^2 \end{aligned} \quad (19)$$

Substituting (19) into (18):

$$\begin{aligned} \dot{V} \leq & -k_1 s^2 - k_2 |s| + |s| \varepsilon_N \\ & - \eta |s| \sum_{i=1}^4 \left( \|\tilde{W}_i\| - \frac{1}{2} \|W\| \right)^2 + \frac{1}{4} \eta |s| \sum_{i=1}^4 \|W_i\|^2 \\ & = -k_1 s^2 - \eta |s| \sum_{i=1}^4 \left( \|\tilde{W}_i\| - \frac{1}{2} \|W\| \right)^2 \\ & - |s| \left( k_2 - \varepsilon_N - \frac{1}{4} \eta \sum_{i=1}^4 \|W_i\|^2 \right) \end{aligned} \quad (20)$$

where  $|\alpha \varepsilon_1 + \beta \varepsilon_3 + \alpha u \varepsilon_2 + \beta u \varepsilon_4| \leq \varepsilon_N$

From (20), if parameter  $k_2$  is designed such that  $k_2 - \varepsilon_N - \frac{1}{4} \eta \sum_{i=1}^4 \|W_i\|^2 > 0$  then  $\dot{V} \leq 0$ .

### 3.2 Stability analysis

**Theorem 1** Consider the closed-loop system with the plant (1), the AHSMC law (15) and the weight updated law for the neural network (17). Then, the second-level sliding surface is asymptotically stable if parameters of control law is designed such that  $k_2 - \varepsilon_N - \frac{1}{4} \eta \sum_{i=1}^4 \|W_i\|^2 > 0$ .

**Proof** Integrating both sides of (18), we obtain:

$$\begin{aligned} \int_0^t dV = & \int_0^t -k_1 s^2 - k_2 |s| \\ & + \eta |s| \sum_{i=1}^4 \tilde{W}_i^T (W_i - \tilde{W}_i) \\ & + s(\alpha \varepsilon_1 + \beta \varepsilon_3 + \alpha u \varepsilon_2 + \beta u \varepsilon_4) dt \end{aligned} \quad (21)$$

Then

$$\begin{aligned} V(0) = & V(t) + \int_0^t -k_1 s^2 - k_2 |s| \\ & - \eta |s| \sum_{i=1}^4 \tilde{W}_i^T (W_i - \tilde{W}_i) \\ & - s(\alpha \varepsilon_1 + \beta \varepsilon_3 + \alpha u \varepsilon_2 + \beta u \varepsilon_4) dt \\ \geq & \int_0^t k_1 s^2 + \eta |s| \sum_{i=1}^4 \left( \|\tilde{W}_i\| - \frac{1}{2} \|W\| \right)^2 \\ & + |s| \left( k_2 - \varepsilon_N - \frac{1}{4} \eta \sum_{i=1}^4 \|W_i\|^2 \right) dt \end{aligned} \quad (22)$$

From (22):

$$\begin{aligned} V(t) \leq & V(0) - \int_0^t k_1 s^2 + \eta |s| \sum_{i=1}^4 \left( \|\tilde{W}_i\| - \frac{1}{2} \|W\| \right)^2 \\ & + |s| \left( k_2 - \varepsilon_N - \frac{1}{4} \eta \sum_{i=1}^4 \|W_i\|^2 \right) dt \\ \leq & V(0) < \infty \end{aligned} \quad (23)$$

$$\text{Therefore, } s \in L_\infty \text{ i.e. } \sup_{t \geq 0} |s| = \|s\|_\infty < \infty \quad (24)$$

Furthermore, from (18) we have:

$$\begin{aligned} |\dot{V}| = & |\dot{s}| |s| \\ \leq & k_1 s^2 + k_2 |s| + \eta |s| \sum_{i=1}^4 \tilde{W}_i^T (W_i - \tilde{W}_i) \\ & + s(\alpha \varepsilon_1 + \beta \varepsilon_3 + \alpha u \varepsilon_2 + \beta u \varepsilon_4) \\ \leq & k_1 s^2 + k_2 |s| + |s| \varepsilon_N \\ & - \eta |s| \sum_{i=1}^4 \left( \|\tilde{W}_i\| - \frac{1}{2} \|W\| \right)^2 + \frac{1}{4} \eta |s| \sum_{i=1}^4 \|W_i\|^2 \\ \leq & k_1 s^2 + k_2 |s| + |s| \varepsilon_N + \frac{1}{4} \eta |s| \sum_{i=1}^4 \|W_i\|^2 \end{aligned} \quad (25)$$

From Eq. (25), it is obvious that  $|\dot{s}| \leq k_1 |s| + k_2 + \varepsilon_N + \frac{1}{4} \eta \sum_{i=1}^4 \|W_i\|^2 < \infty$ , hence  $\dot{s} \in L_\infty$

$$\text{i.e. } \sup_{t \geq 0} |\dot{s}| = \|\dot{s}\|_\infty < \infty \quad (26)$$

From (22), we obtain:

$$\begin{aligned}
 V(0) &\geq \int_0^\infty \left( k_1 s^2 + \eta |s| \sum_{i=1}^4 \left( \|\tilde{W}_i\| - \frac{1}{2} \|W\| \right)^2 \right. \\
 &\quad \left. + |s| \left( k_2 - \varepsilon_N - \frac{1}{4} \eta \sum_{i=1}^4 \|W_i\|^2 \right) \right) dt \\
 &= \int_0^\infty |s| \left( k_2 - \varepsilon_N - \frac{1}{4} \eta \sum_{i=1}^4 \|W_i\|^2 \right) dt \\
 &\quad + \int_0^\infty k_1 s^2 dt + \int_0^\infty \eta |s| \sum_{i=1}^4 \left( \|\tilde{W}_i\| - \frac{1}{2} \|W\| \right)^2 dt
 \end{aligned} \quad (27)$$

It is obvious that:

$$\int_0^\infty k_1 s^2 dt \geq 0, \int_0^\infty |s| \left( k_2 - \varepsilon_N - \frac{1}{4} \eta \sum_{i=1}^4 \|W_i\|^2 \right) dt \geq 0$$

and  $\int_0^\infty \eta |s| \sum_{i=1}^4 \left( \|\tilde{W}_i\| - \frac{1}{2} \|W\| \right)^2 dt \geq 0$ .

Hence, from Eq. (27) we have:  $\int_0^\infty |s| dt < \infty$ ,

$$\text{i.e. } \|s\|_1 < \infty \text{ and } \int_0^\infty s^2 dt < \infty, \text{ i.e. } s \in L_2 \quad (28)$$

Since  $s \in L_\infty$ ,  $\dot{s} \in L_\infty$  and  $s \in L_2$ , due to Barbalat's lemma we have  $\lim_{t \rightarrow \infty} s = 0$ . Therefore the second-level sliding surface  $s$  is asymptotically stable.

**Theorem 2** [19]: Consider the closed-loop system with a stable equilibrium point consisting of the plant (1), the AHSMC law (15) and the weight updating law of neural network (17). It is assumed that  $s_2$  and  $\dot{s}_2$  are bounded (i.e.  $s_2 \in L_\infty$  and  $\dot{s}_2 \in L_\infty$ ). Then, we have that first-level sliding surfaces  $s_1$  and  $s_2$  are asymptotically stable if parameters of control law is designed such that  $k_2 - \varepsilon_N - \frac{1}{4} \eta \sum_{i=1}^4 \|W_i\|^2 > 0$ .

**Proof** Due to  $\sup_{t \geq 0} |s| = \|s\|_\infty < \infty$ ,  $\sup_{t \geq 0} |\dot{s}| = \|\dot{s}\|_\infty < \infty$ , and the assumption that  $\sup_{t \geq 0} |s_2| = \|s_2\|_\infty < \infty$ ,  $\sup_{t \geq 0} |\dot{s}_2| = \|\dot{s}_2\|_\infty < \infty$ , we obtain  $\sup_{t \geq 0} |s_1| = \|s_1\|_\infty < \infty$ ,  $\sup_{t \geq 0} |\dot{s}_2| = \|\dot{s}_2\|_\infty < \infty$ .

From the derivation of control design, we find that  $\alpha, \beta$  do not influence the stability of the closed-loop system, if  $k_2 - \varepsilon_N - \frac{1}{4} \eta \sum_{i=1}^4 \|W_i\|^2 > 0$  is satisfied.

Hence, we can construct two sliding surfaces as follows:

$$S_1 = (\alpha_1 s_1 + \beta s_2), \quad S_2 = (\alpha_2 s_1 + \beta s_2) \quad (29)$$

where  $\alpha_1, \alpha_2$  are arbitrary positive constants and  $\alpha_1 \neq \alpha_2$ . Because the roles of  $S_1$  and  $S_2$  are identical, we can suppose that  $\infty > \int_0^\infty S_1^2 dt > \int_0^\infty S_2^2 dt \geq 0$ . From Eq. (29), we obtain:

$$\begin{aligned}
 0 &\leq \int_0^\infty S_1^2 dt \\
 &= \int_0^\infty (\alpha_1^2 s_1^2 + 2\alpha_1 \beta s_1 s_2 + \beta^2 s_2^2) dt < \infty
 \end{aligned} \quad (30)$$

$$\begin{aligned}
 0 &\leq \int_0^\infty S_2^2 dt \\
 &= \int_0^\infty (\alpha_2^2 s_1^2 + 2\alpha_2 \beta s_1 s_2 + \beta^2 s_2^2) dt < \infty
 \end{aligned} \quad (31)$$

Hence,

$$\begin{aligned}
 0 &< \int_0^\infty (S_1^2 - S_2^2) dt \\
 &= \int_0^\infty (\alpha_1^2 - \alpha_2^2) s_1^2 + 2(\alpha_1 - \alpha_2) \beta s_1 s_2 dt \\
 &= \int_0^\infty (\alpha_1^2 - \alpha_2^2) s_1^2 \\
 &\quad + 2(\alpha_1 - \alpha_2) \beta s_1 (S_1 - \alpha_1 s_1) dt \\
 &= \int_0^\infty -(\alpha_1 - \alpha_2)^2 s_1^2 dt + \int_0^\infty 2(\alpha_1 - \alpha_2) \beta s_1 S_1 dt
 \end{aligned} \quad (32)$$

From (32) we obtain:

$$\begin{aligned}
 \int_0^\infty (\alpha_1 - \alpha_2)^2 s_1^2 dt &< \int_0^\infty 2(\alpha_1 - \alpha_2) s_1 S_1 dt \\
 &\leq \int_0^\infty |2(\alpha_1 - \alpha_2) s_1 S_1| dt \\
 &\leq 2|\alpha_1 - \alpha_2| \int_0^\infty \|s_1\|_\infty |S_1| dt \\
 &= 2|\alpha_1 - \alpha_2| \|s_1\|_\infty \|S_1\|_1 < \infty
 \end{aligned} \quad (33)$$

$$\text{Therefore, } \int_0^\infty s_1^2 dt < \infty \quad (34)$$

Because  $s_1 \in L_\infty$ ,  $\dot{s}_1 \in L_\infty$ , and  $s_1 \in L_2$  according to Barbalat's lemma we have  $\lim_{t \rightarrow \infty} s_1 = 0$ . Similarly,  $\lim_{t \rightarrow \infty} s_2 = 0$ .

Therefore all first-level sliding surfaces  $s_1$  and  $s_2$  are asymptotically stable.

**Comment** [19]: For underactuated systems with stable equilibrium like overhead crane, the assumption that  $s_2 \in L_\infty$  and  $\dot{s}_2 \in L_\infty$  can easily be satisfied.

## 4 Simulation and experiment results

In this section, the HSMC and AHSMC methods are verified by simulation and experiments with the actual model of 2D overhead crane in laboratory. The real object in laboratory is shown in Fig. 2.





**Fig. 2** The 2D overhead crane control system in laboratory

The physical parameters of the real overhead crane are given as follows:  $M = 25$  kg,  $m = 8$  kg,  $l = 1.2$ ,  $g = 9.81$ . The parameters of HSMC law are selected as:  $c_1 = 3$ ,  $c_2 = 0.01$ ,  $\alpha = 2$ ,  $\beta = 1.4$ ,  $k_1 = 0.1$ ,  $k_2 = 2$ . The RBF network is constructed with the usage of 200 nodes, where the input  $X = [\theta \ \dot{\theta}]^T$ , the centers  $\mu_i$  are evenly spaced on  $\mu_i = [-1.2, 1.2] \times [-1.6, 1.6]$  and the widths  $\varsigma_i = 0.8$ , for  $i = 1, 2$ . The adaptive parameters are designed as  $F_i = 0.1$ ,  $\eta = 3$ , the initial weight matrices  $\hat{W}_i(0)$  are all equal to 0.1.

#### 4.1 Simulation results

The simulation results of the AHSMC method in comparison with those of the HSMC law are shown in Figs. 3, 4 and 5, respectively. These figures show the position of trolley, the swing angle of payload, and the control force, respectively. Table 1 indicates comparison detail of controllers using HSMC and AHSMC law.

According to the Table 1, it is clear that both the HSMC and AHSMC schemes ensure the quality of the overhead crane, in which performance of the HSMC method shows better performance in comparison with that of the AHSMC law. However, the design process of the AHSMC does not

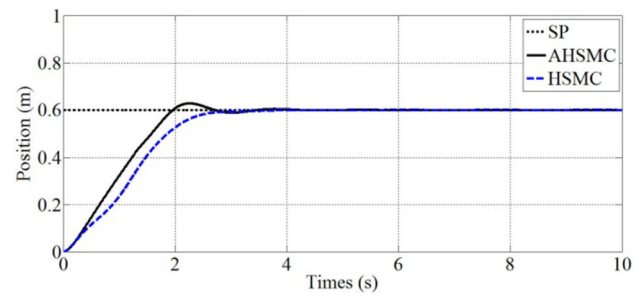


**Fig. 3** Position of trolley

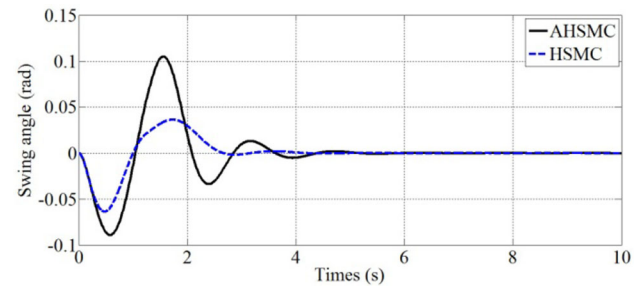


**Fig. 4** Swing angle of payload

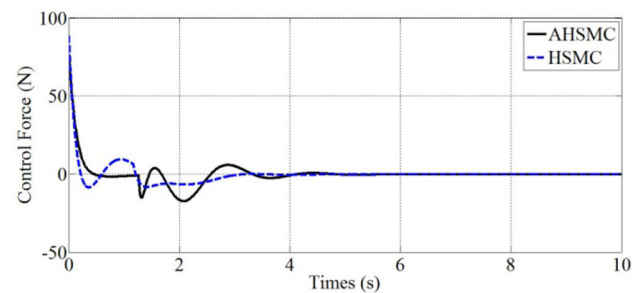


**Fig. 5** Control force

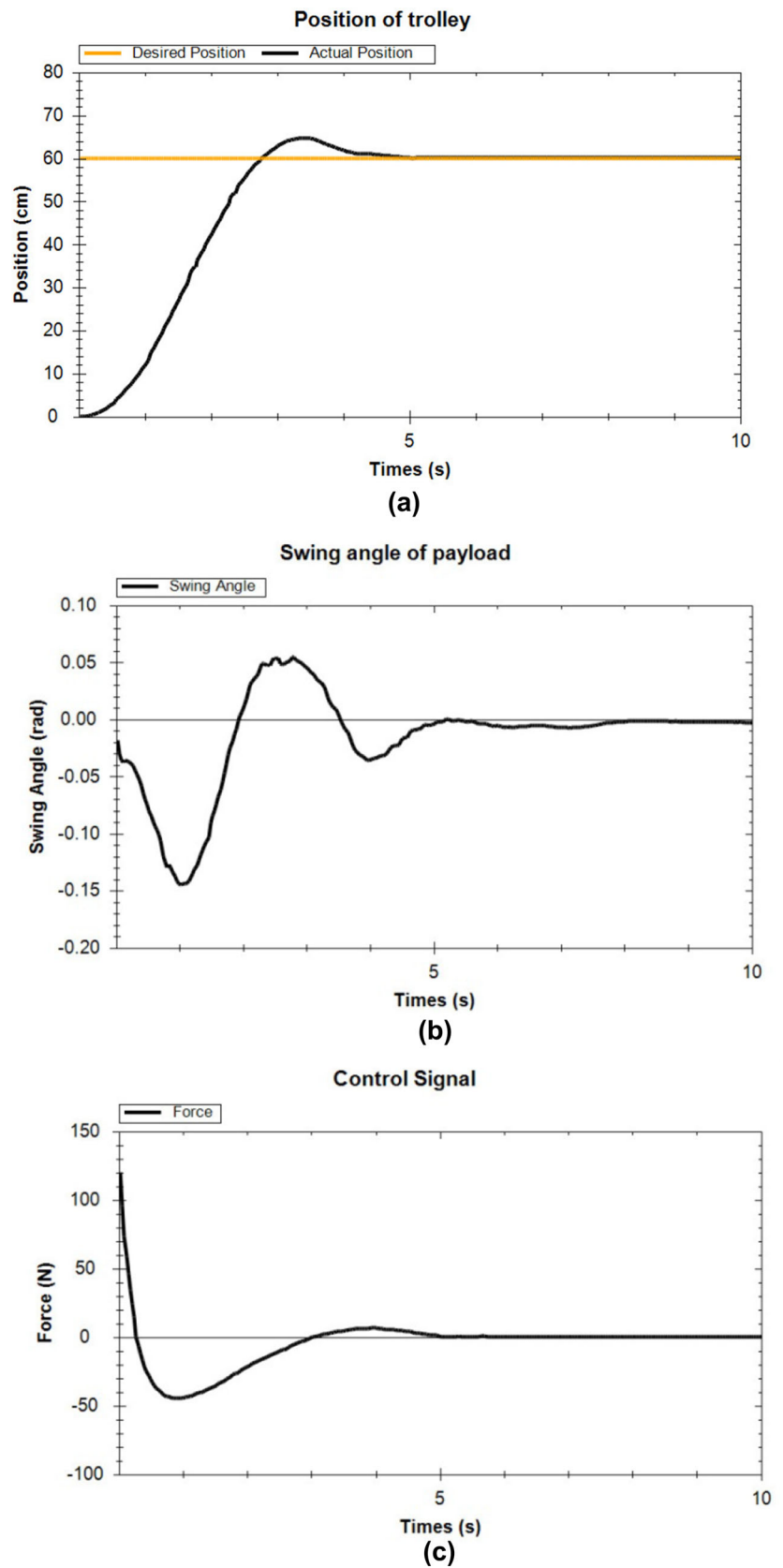
**Table 1** Comparison of the HSMC and AHSMC laws

	HSMC	AHSMC
Settling time (s)	4	4
Overshoot (%)	0	5
Maximum angle (rad)	0.065	0.1

require full information of the crane's model, which is difficult to achieve in practice.

Based on simulation results, the AHSMC law is installed on the microcontroller for the prototype in the laboratory. A digital controller is constructed on STM32F4 microcontroller, the trolley is driven by a three-phase asynchronous motor and the inverter 3G3JX, the position and the velocity of the trolley are measured by the encoder E40S6-1024-3-T-24, the swing angle and the angular velocity of payload are gained by the sensor MPU6050. The experiment result for the AHSMC method is shown in Fig. 6.

**Fig. 6** Experiment result for AHSMC law **a** Position of trolley. **b** Swing angle of payload. **c** Control force





As can be seen from the Fig. 6, the trolley arrived at the expected position in nearly 5 s and the absolute value of the angle of the payload is less than 0.15 rad. Therefore, the digital controller using AHSMC law has good performance in the actual environment which contains external disturbances and parametric uncertainties.

## 5 Conclusion

This paper has proposed an adaptive control scheme for the 2-D uncertain overhead crane based on hierarchical sliding mode control structure. The radial basis function neural network is applied to constitute an adaptive mechanism for estimating the unknown dynamics. The stability of sliding surfaces in all layers are proven by using the Lyapunov theory and Barbalat's lemma. Both simulation and experimental results verify that the controller is effective to move the trolley with smaller payload oscillation. In addition, as there is no requirement about an adequate description of the plant, the presented controller is possibly applied capable in numerous different industrial applications.

## References

1. Fang Y, Zergeroglu E, Dixon WE, Dawson DM (2003) Nonlinear coupling control laws for an overhead crane system. *IEEE/ASME Trans Mechatron* 8(3):418–423
2. Yu J, Lewis FL, Huang T (1995) Nonlinear feedback control of a gantry crane. In: *Proceedings of 1995 American control conference*, pp 4310–4315
3. Park H, Chwa D, Hong K (2007) A feedback linearization control of container cranes: varying rope length. *Int J Control Autom Syst* 5(4):379
4. Tuan LA, Kim GH, Lee SG (2012) Partial Feedback linearization control of the three dimensional overhead crane. In: *IEEE International Conference on Automation Science and Engineering*, pp 1198–1203
5. Le TA, Kim GH, Kim MY, Lee SG (2012) Partial feedback linearization control of overhead cranes with varying cable lengths. *Int J Precis Eng Manuf* 13(4):501–507
6. Cho S-K, Lee H-H (2002) A fuzzy-logic anti-swing controller for three-dimensional overhead cranes. *ISA Trans* 41(2):235–243
7. Mahfouf M, Kee CH, Abbod MF, Linkens DA (2000) Fuzzy logic-based anti-sway control design for overhead cranes. *Neural Comput Appl* 9(1):38–43
8. Wang L, Zhang H, Kong Z (2015) Anti-swing control of overhead crane based on double fuzzy controllers. In: *Proceedings of 27th Chinese Control Decision Conference*, pp 981–986
9. Shyu KK, Jen CL, Shang LJ (2005) Design of sliding-mode controller for anti-swing control of overhead cranes. In: *31st Annual Conference of IEEE Industry Electronics Society*, pp 147–152
10. Qian D, Yi J, Zhao D (2011) Control of overhead crane systems by combining sliding mode with fuzzy regulator. *IFAC Proc* 44(1):9320–9325
11. Tuan LA, Kim JJ, Lee SG, Lim TG, Nho LC (2014) Second-order sliding mode control of a 3D overhead crane with uncertain system parameters. *Int J Precis Eng Manuf* 15(5):811–819
12. Ngo QH, Hong KS (2012) Sliding-mode anti-sway control of an offshore container crane. *IEEE/ASME Trans Mechatron* 17(2):201–209
13. Bartolini G, Pisano A, Usai E (2002) Second-order sliding-mode control of container cranes. *Automatica* 38(10):1783–1790
14. Xu W, Zheng X, Liu Y, Zhang M, Luo Y (2015) Adaptive dynamic sliding mode control for overhead cranes. In: *Proceedings of the 34th Chinese Control Conference*, pp 3287–3292
15. Wang W, Yi J, Zhao D, Liu D (2004) Design of a stable sliding-mode controller for a class of second-order underactuated systems. *IEEE Proc Control Theory Appl* 151(6):243–250
16. Qian D, Yi J, Zhao D (2008) Hierarchical sliding mode control for a class of SIMO underactuated system. *Control Cybern* 37(1):160–175
17. Wang W, Liu XD, Yi JQ (2007) Structure design of two types of sliding-mode controllers for a class of under-actuated mechanical systems. *IET Control Theory Appl* 1(1):163–172
18. Qian D, Liu X (2012) Adaptive control based on hierarchical sliding mode for under-actuated systems. *Appl Math Inf Sci* 1364(4):1050–1055
19. Singh AM, Hoang VT, Ha QP (2016) Fast terminal sliding mode control for gantry cranes. In: *International symposium on automation and robotics in construction*
20. Tuan LA, Lee S-G, Nho LC, Kim DH (2013) Model reference adaptive sliding mode control for three dimensional overhead cranes. *Int J Precis Eng Manuf* 14(8):1329–1338
21. Yang JH, Yang KS (2007) Adaptive coupling control for overhead crane systems. *Mechatronics* 17(2–3):143–152
22. Ji G (2012) Adaptive neural network dynamic surface control for perturbed nonlinear time-delay systems. *Int J Autom Comput* 9(April):135–141
23. Park MS, Chwa D, Hong SK (2008) Anti-sway tracking control of overhead cranes with system uncertainty and actuator nonlinearity using an adaptive fuzzy sliding-mode control. *IEEE Trans Ind Electron* 55(11):3972–3984
24. Park M, Chwa D, Eom M (2014) Adaptive sliding-mode anti-sway control of uncertain overhead cranes with high-speed hoisting motion. *IEEE Trans Fuzzy Syst* 22(5):1262–1271
25. Hung LC, Chung HY (2007) Decoupled control using neural network-based sliding-mode controller for nonlinear systems. *Expert Syst Appl* 32(4):1168–1182
26. Hung LC, Chung HY (2007) Decoupled sliding-mode with fuzzy-neural network controller for nonlinear systems. *Int J Approx Reason* 46(1):74–97
27. Huang S-J, Huang K-S, Chiou K-C (2003) Development and application of a novel radial basis function sliding mode controller. *Mechatronics* 13(4):313–329
28. Nguyen NP, Ngo QH, Nguyen CN (2017) Adaptive sliding mode control using radial basis function network for container cranes. In: *2017 17th international conference on control, automation and systems*, pp 1628–1633